SC-R-67-1028
December 1967

IMPACT TECHNIQUES FOR THE STUDY OF PHYSICAL PROPERTIES OF SOLIDS UNDER SHOCK-WAVE LOADING

R. A. Graham

SANDIA LABORATORIES

OPERATED FOR THE U. S. ATOMIC ENERGY COMMISSION BY SANDIA CORPORATION | ALBUQUERQUE, NEW MEXICO; LIVERMORE, CALIFORNIA

Issued by Sandia Corporation,
a prime contractor to the
United States Atomic Energy Commission

Impact Techniques for the Study of Physical Properties of Solids Under Shock-Wave Loading[1]

R. A. GRAHAM

Sandia Laboratory, Albuquerque, N. M.
Assoc. Mem. ASME

Measurements of various physical properties of solids while they are subjected to shock-wave loading from precisely aligned projectile impacts are described in order to illustrate the unique features and capabilities of the impact experiment. Results and experimental techniques are shown for the measurements of: (1) the piezoelectric coefficient of X-cut quartz from 2.6 to 25 kbar, (2) the permittivity change of 60 deg orientation sapphire from 20 to 100 kbar, (3) the resistance of [111] germanium which gives resistivity data in the elastic range and permits identification of the solid-solid phase transition at about 120 kbar, and (4) the compressibility of ferromagnetic fcc 30 Ni-70 percent Fe from 4 to 50 kbar which permits identification of the pressure-induced Curie point transition and a complete thermodynamic description of the transition.

Introduction

Measurements of the characteristics of shock-waves in solids have been used for many years in the study of compressibilities under high pressure. In fact, shock-wave data are still the major source for compressibility data of solids above 100 kbar. There have been a number of review articles [1–6][2] which describe the shock-wave compression experiments and results which are typical when high explosive loading is used to produce the shock wave. Recently, however, new experimental apparatus and techniques have been developed for performing shock-wave experiments in which the impact of flat-faced projectiles produces the shock waves. Many of the characteristics of impact experiments are fundamentally different from explosive loading experiments and they permit significantly different experimental arrangements which allow additional measurements to be made. A number of well-defined, precise measurements of various physical properties have now been performed with impact techniques. These measurements have demonstrated that the impact experiment is particularly well suited for the measurement of physical properties under shock-wave loading.

It is the purpose of this paper to describe several measurements of physical properties of solids under shock-wave loading as obtained with impact techniques. It is intended that these descriptions will demonstrate the unique capabilities of the impact experiment which previous review articles concerning shock waves in solids have largely neglected.

Following a brief review of characteristics of shock waves in solids, the general features of impact experiments will be shown. The results of specific measurements of different physical properties will then be presented to illustrate the various experimental arrangements and techniques.

Characteristics of Shock Waves in Solids

Besides the obvious differences in rates of loading and thermodynamic conditions between shock-wave loading and static high pressure experiments, one of the more basic differences is that the stress or pressure[3] experienced by the sample in a shock-wave loading experiment is a direct result of the inertial response of the sample to the externally applied loading. Thus, different materials subjected to identical loading arrangements experience uniquely different pressure amplitude and pressure versus time histories which, in turn, depend upon their stress-volume behavior. Hence, it is essential to consider the interdependence of the stress-volume relation and the experimentally observable characteristics of shock waves.

Consider a plane compressive shock-wave propagating through a solid in response to a rapidly applied impulsive load at one plane boundary of the sample. The passage of the shock wave imparts a stress, σ, and a particle velocity, u, in the direction of propagation. Assuming that all stress components travel with the same shock velocity, U, the conservation of momentum relation gives

$$\sigma = \rho_0 U u, \tag{1}$$

where ρ_0 is the density of the solid ahead of the front. Further, from the conservation of mass

$$V/V_0 = 1 - \frac{u}{U}, \tag{2}$$

where V_0 is the specific volume $\left(\frac{1}{\rho_0}\right)$ of the unstressed material and V is the specific volume of the stressed material.[4] It is evident from equations (1) and (2) that the simultaneous measurement of values of the shock velocity, U, and the particle velocity, u, characterizes the stress and volume of the material under shock-wave compression and shock-wave compressibility experiments are directed toward their determination.

A schematic diagram of a conventional shock-wave experiment to measure the compressibility of solids with explosive loading is shown in Fig. 1. A plane shock wave is produced by the deto-

---

[1] This work was supported by the United States Atomic Energy Commission.

[2] Numbers in brackets designate References at end of paper.

Contributed by the Research Committee on Pressure Technology and presented at the Winter Annual Meeting, New York, N. Y., November 27–December 1, 1966, of The American Society of Mechanical Engineers. Manuscript received at ASME Headquarters, August 1, 1966. Paper No. 66—WA/PT-2.

[3] A plane shock wave produces a one-dimensional compression in the direction of shock propagation. Hence, while the solid offers shear resistance, the stress configuration is not hydrostatic. When the terminology "pressure" is used, it will imply that the stress configuration can be considered hydrostatic; otherwise the more precise term "stress" will be used.

[4] Equations (1) and (2) describe a shock wave moving into an unstressed medium which is at rest. In the event multiple shock waves are propagating, the stress and particle velocity shown should be considered as the change across a particular wave front and the shock velocity should be taken relative to the medium ahead of the front.

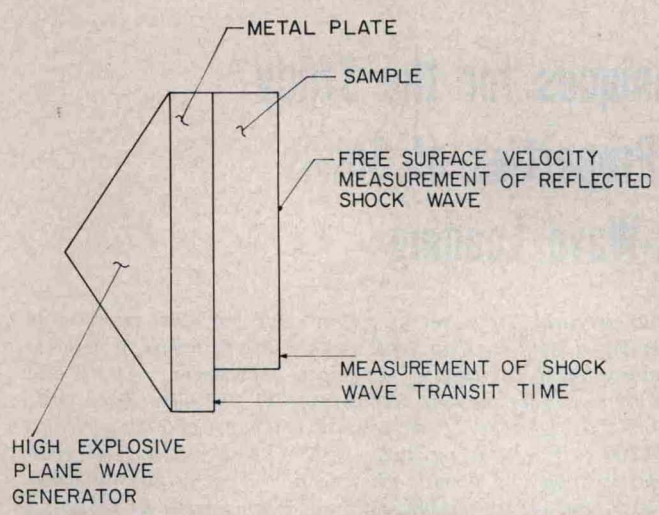

Fig. 1 Schematic drawing of a direct contact explosive loading experiment to determine compressibility

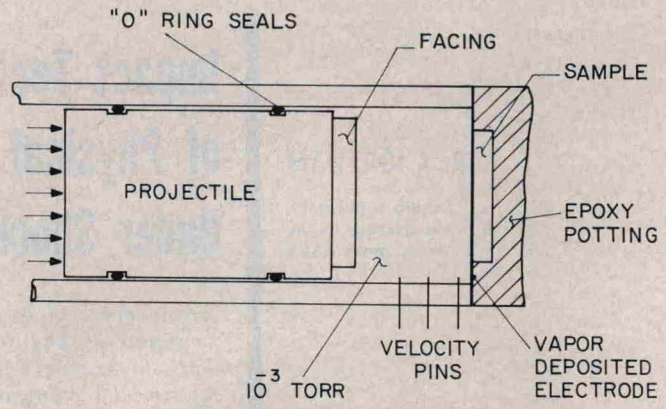

Fig. 2 Typical arrangement of an impact experiment

nation of a high explosive plane-wave lens. This shock-wave is transmitted through a metal plate (typically aluminum) into the sample. Measurement of the transit time of the shock-wave through a known thickness of the sample allows the shock velocity, U, to be computed. After the shock wave traverses the sample, it impinges upon and reflects from a plane parallel surface (called the free-surface) causing this surface to move with a velocity which, to a very close approximation, is equal to twice the particle velocity of the incident wave. The measurement of the free-surface velocity is accomplished by various optical and electronic techniques [7, 8] and is more difficult and less precise than the shock velocity measurement. There are numerous variants of this experimental arrangement but all are directed toward shock-wave velocity and free-surface velocity measurements.

When it is desired to measure the change in some physical property, other than compressibility, resulting from the shock-wave compression, the experimental arrangement of Fig. 1 has some shortcomings. Whereas the end result desired in compressibility measurements is the U versus u data, other physical property experiments require the U, u data as the independent variable to specify the stress and volume for which physical change is measured. Large unacceptable uncertainties often result if nominal values are assumed for U and u. Further, it is difficult to arrange precise simultaneous measurements of U, u in addition to the physical property change. On the other hand, impact experiments seem to have particularly advantageous features for the measurement of physical properties under shock-wave loading.

General Features of Impact Experiments

The impact experiment is conceptually simple but requires that certain exacting experimental conditions be satisfied in order to perform a satisfactory experiment. The principle features of an impact experiment are illustrated in Fig. 2.

The impact of the precisely aligned plane surfaces of two disks is produced by accelerating the impacting disk to various velocities in a smooth bore gun. Perhaps the most convenient and effective method for accelerating the projectile is compressed gas [9–13] although propellants [14–16] have also been employed. The impacting disk is normally attached as a facing on the main body of the projectile. To achieve the precise alignment required, the specimen is attached to the muzzle of the gun such that the impact occurs while the projectile is guided by the accurately machined gun bore.

The allowable values for the angular misalignment between the impacting surfaces (called "tilt") vary with the nature of the experiment and the impact velocity. It is necessary for the impacting surfaces to close in times short compared to the time for the shock wave to traverse the sample. Thus, experiments at low impact velocities require smaller values of tilt than experiments at high impact velocity and the techniques employed for alignment are designed to give acceptable values for tilt at low impact velocities. Generally, an average value for tilt of about 5×10^{-4} radian is satisfactory for the type of experiments to be described. Various investigators have used different means to achieve the precisely aligned impact and the technology for achieving this is reasonably widespread although principally utilized for the measurement of mechanical properties.[5] If provisions for securing low values of tilt are not made, meaningful measurements are not possible in the particularly important low velocity (low stress) region. Further, it is important to compare shock-wave measurements in their low pressure limit to atmospheric pressure values. Thus, exclusion of the low stress region is a serious experimental limitation.

To prevent air pressure buildup between the rapidly closing surfaces of the facing and specimen, it is necessary to evacuate the space between the projectile and specimen to a pressure of about 10^{-3} torr. The high pressure driving the projectile is sealed from the vacuum by "O" ring seals on the projectile.

As will be demonstrated later, one of the most useful measurements made in an impact experiment is that giving the velocity of the impacting surface. For the impact of like materials, this velocity measurement gives additional data to that which can be obtained in an explosive loading experiment and much of the effectiveness of the impact experiment is lost if the provision for velocity measurements is not made. The most precise measurements are made with electrical discharge contact pins which may protrude either through the side of the gun bore [17] or through the plane of the specimen toward the projectile [18]. The velocity of the impacting disk at the instant of impact can typically be measured to ± 0.5 percent.

Measurements of the electrical behavior of the specimen usually require a conducting electrode at the impact surface. To maintain precise alignment and provide minimum distortion to the shock wave, the electrode is normally a thin vapor deposited layer of aluminum or silver.

Although not absolutely essential, the effectiveness of the experiment is greatly enhanced if a preselected impact velocity can be achieved within about 5 percent of the desired velocity. Even though the velocity is to be precisely measured on each experiment there are numerous instances for which experiments are required in the neighborhood of a critical point. Further, this control results in the capability of achieving virtually continuous

[5] Impact techniques are also effectively employed for the measurement of mechanical properties. Since many of the alignment techniques and other experimental problems are similar, a supplementary list of references on mechanical property measurements by impact techniques is included at the end of the individually cited references.

value stress over a range of stress which can be quite large.[6]

In summary, an impact experiment suitable for well-defined physical property measurements has the following general features:

1 Precise alignment of the impacting surfaces of facing and specimen disks
2 Provisions for impact in vacuum
3 Precise measurement of velocity at impact
4 Capability of obtaining a preselected impact velocity

The Impact Relationships

If the impact of two flat surfaces is achieved under the conditions described above, the particle velocity imparted to the specimen as a result of the impact can be precisely determined. The relations that specify the impact conditions follow from the consideration that for all times when the impacting and impacted surfaces are in contact, the stress and particle velocity must have the same values across the interface. Thus, it follows that:

$$U_0 - u_a = u_b \tag{3}$$

and

$$\sigma_a = \sigma_b \tag{4}$$

where U_0 is the impact velocity, u is the particle velocity, and σ is the stress in the impact direction imparted to the facing. The subscript a refers to the facing and b refers to the specimen. Combining these relations with equation (1) results in the relation:

$$u_b = \frac{Z_a}{Z_a + Z_b} U_0 \tag{5}$$

where Z represents the shock-wave impedance ($\rho_0 U$) for the stress and particle velocity of the experiment.[7] Thus, if the properties of the facing and specimen are known, the particle velocity can be computed from the measured impact velocity. In general, however, these properties are unknown or not known with sufficient precision so that it is difficult to perform precise experiments with dissimilar materials impacting upon each other.

However, if the facing and specimen are the same material, equation (5) is greatly simplified since

$$u_a = u_b = u = (1/2)U_0. \tag{6}$$

For this condition the particle velocity imparted to the target is precisely known regardless of the material used or whether its properties are known. The impact of identical materials, termed the symmetric impact, is clearly the best defined condition for use in impact experiments and is utilized in the major portion of the work to be presented.

Physical Property Measurements

Impact techniques are best illustrated by describing specific methods employed for various measurements. Some of these measurements are reported here for the first time while others are reported in more detail elsewhere and are shown here only to illustrate particular features of technique.

Piezoelectric Properties of X-cut Quartz [19, 23]

The most extensive measurements accomplished to date have been made to determine the piezoelectric properties of X-cut quartz (references [19–23]) under shock-wave compression. As illustrated in Fig. 3, both facing and specimen are disks of X-cut quartz. For a given experiment the velocity of the impacting disk is measured along with the short-circuited current which results from the shock wave traversing the specimen disk. Previously it was demonstrated [23] that this current, i, produced by the piezoelectric effect is:

$$i = f_{11} \frac{\sigma A U}{l}, \qquad 0 < t < l/U \tag{7}$$

where f_{11} is the piezoelectric coefficient relating the component of stress to the resulting charge on the x-face; A is the area of the disk; σ is the x-component of stress; l is the thickness of the disk, and t is the time. In the low signal limit, $f_{11} = e_{11}/c_{11}$, where e_{11} is the piezoelectric stress constant and c_{11} is the elastic stiffness constant. It is apparent from equations (6), (7), and (1) that measurements of U and U_0 along with the resulting current and predetermined dimensions of the disk are sufficient to determine the piezoelectric coefficient.

A typical current-time oscilloscope trace is shown in Fig. 4.

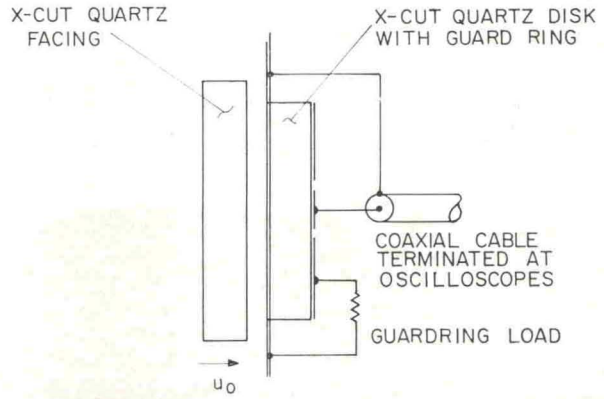

Fig. 3 Experimental arrangement for the measurement of the piezoelectric coefficient. The guard ring geometry is employed to obtain one-dimensional conditions.

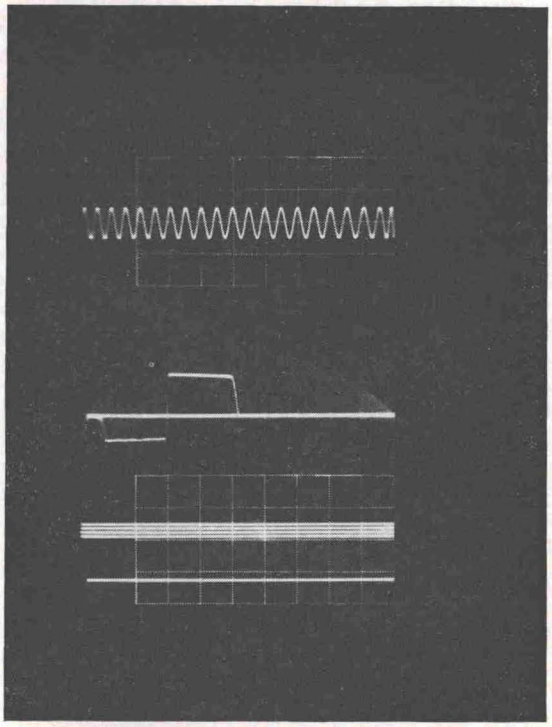

Fig. 4 Typical current-time record from impact loaded quartz. A timing wave of 10 Mc is shown at the top and the amplitude calibration is below the signal. Time increases from right to left. The positive signal corresponds to the transit of the wave through the crystal. The negative signal is that due to the reflected wave from the rear of the specimen.

[6] The author has performed experiments from 2.5 to 450 kbar with the gun described in reference [11].

[7] In general, the impedance of the solid will depend upon the stress; thus a graphical solution would be employed for the particle velocity rather than the analytical method implied by equation (5). See reference [2], p. 179.

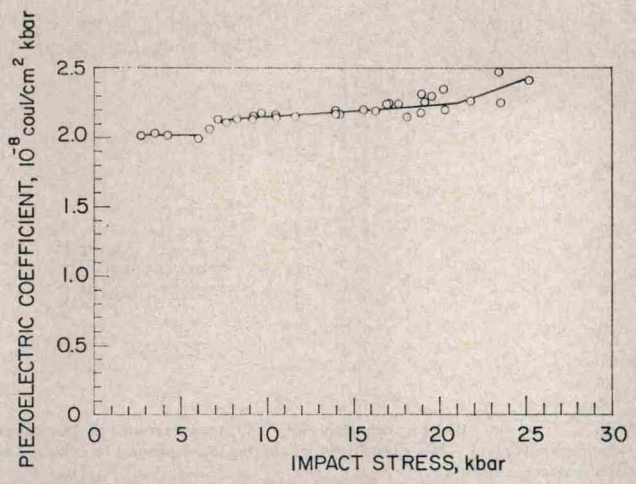

Fig. 5 The piezoelectric coefficient of X-cut quartz under shock-wave compression. These data should not be confused with the previously reported current coefficient which is employed when quartz is used as a gage [23].

The record not only shows the current amplitude but also the time taken for the shock wave to traverse the known thickness of the specimen disk. From this measured transit time and the measured impact velocity, the particle velocity and shock velocity are precisely specified on each experiment. This method of measuring the shock velocity has the desirable feature of an intimate connection between the measurements of the shock-wave amplitude and the resulting piezoelectric polarization. Since both shock velocity and current are measured from the same record, any peculiarities in response such as a transient rate effect have a direct observable effect on both quantities.

Equation (7) was derived assuming infinitesimal strain and no permittivity change. As shown in the typical record, the current actually increases slightly in time which can be shown to be the result of the strain, electromechanical coupling, and a slight increase in permittivity. The solutions for the effect of these variables on the current [23] show that the current at one-half transit time is, for the conditions of our experiments, equal to that expected from equation (7). Hence, this current is a measure of the piezoelectric coefficient, f_{11}. Values obtained for f_{11} are shown in Fig. 5. Note that a typical increment of stress is about 2 kbar and that in the vicinity of 6 and 18 kbar, 1 kbar increments are achieved. The lowest stress point is within the previously reported [24] region of constant piezoelectric response.

In the low signal limit when a small correction is made for the area of the insulating ring, the data show a value for e_{11}/c_{11} of 2.01×10^{-8} coul/cm^2 kbar which is in excellent agreement with the value of 2.02×10^{-8} coul/cm^2 kbar by Koga, et al. [27] and 1.97 coul/cm^2 kbar by Bechmann [28].

The relations given in equations (1) and (2) describe the propagation of single shock waves. Frequently, a slope discontinuity or cusp exists in the stress-volume relation as a result of exceeding the Hugoniot elastic limit[8] or inducing a phase transition. For stresses in excess of the amplitude of the cusp it is possible for two waves to propagate at distinctly different shock velocities and in order to properly interpret the data, it is essential to determine if multiple wave fronts exist. The Hugoniot elastic limit of X-cut quartz has been found to be about 50 kbar [25, 26].

As the stress approached the Hugoniot elastic limit and beyond, it was not possible to obtain a satisfactory analytical expression for quantitative data reduction. Hence, even though this experiment was performed to about 150 kbar, no results are reported in the vicinity of the Hugoniot elastic limit.

For these measurements the reproducibility of the impact conditions was found to be particularly useful. It was possible to look extensively at the effects of deviations from one-dimensional conditions resulting from the geometry of the specimen. These effects produce distortions to the current-time waveforms which are similar to the effects of permittivity change. Thus, they are a potential source of error unless carefully investigated.

Recently, impact techniques have been used to determine the piezoelectric coefficient, f_{11}, under shock-wave compression at liquid nitrogen temperatures [29]. Also, the current produced from impacted ferroelectrics has recently been measured and analyzed [30].

[8] The Hugoniot elastic limit is the stress amplitude corresponding to the cusp in the stress-volume relation resulting from the transition between elastic and plastic compression under the one-dimensional strain conditions of shock-wave loading.

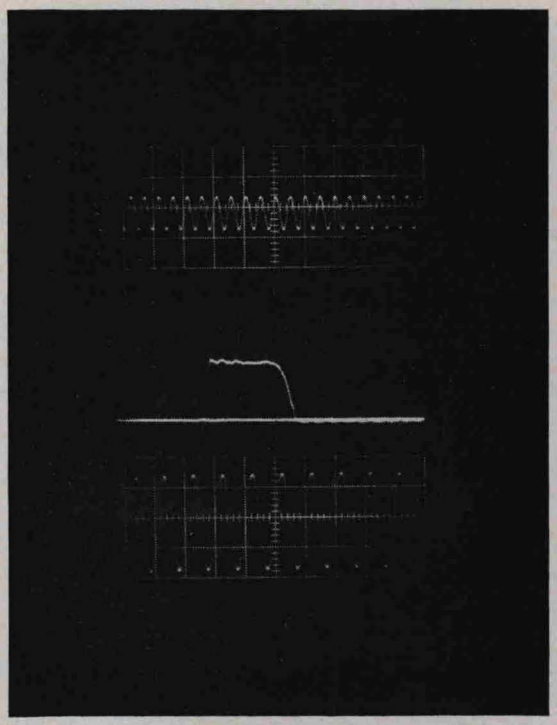

Fig. 6 Typical current time record due to the permittivity change induced by shock wave of 32 kbar. A timing wave of 20 Mc is shown at the top and the amplitude calibration is below the signal. The signal amplitude is about 8.5×10^{-4} amp with a 32-mm dia disk 3.2 mm thick. An electrostatic potential of 730 volts was applied to the specimen.

Permittivity of Sapphire Under Shock-Wave Compression

An experimental arrangement similar to that used for quartz has been used to measure the permittivity change induced in sapphire by shock-wave compression. Here the shock wave is induced in the specimen by the symmetrical impact of sapphire disks [31]. If an electrostatic potential is applied to the specimen disk, a current flows in an external short-circuit due to the capacitance change induced by the shock wave. This capacitance change results from two effects: the strain and the stress induced permittivity change. For conditions of infinite resistivity, one-dimensional strain, and electric field, small strains and small permittivity changes, it can be shown that the short-circuited current is given by:

$$i = \frac{VAU\epsilon_0}{l^2}\left[\frac{\Delta\epsilon}{\epsilon_0} + \frac{u}{U}\right], \qquad 0 < t < l/u \tag{8}$$

where V is the electrostatic potential on the disk, $\Delta\epsilon$ is the change in permittivity, and ϵ_0 is the unstressed permittivity. It is evident from equation (8) that if values of U and u are obtained along with the resulting current, the permittivity change can be computed. The experiment consists of the symmetrical impact of sapphire disks and a measurement of the resulting current-time pulse. A typical record is shown in Fig. 6. Note that as was the case with the quartz experiments, the current-time trace indicates the time for the shock wave to traverse the disk and thus provides

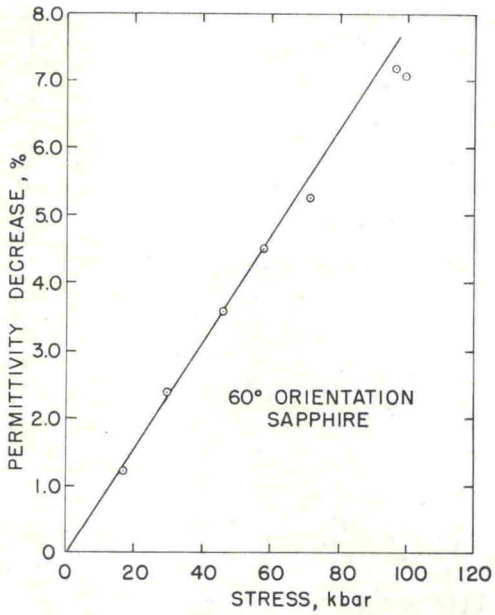

Fig. 7 Permittivity change of sapphire under shock-wave compression as computed from equation (8)

the data necessary to compute the shock velocity. The particle velocity is determined from the measured impact velocity according to equation (6).

To measure the Hugoniot elastic limit, which determines the limit of the elastic wave region, subsidiary experiments were performed with explosive loading [32]. The observed values depend upon the total pressure imparted to the sample and the crystalline orientation and vary from 120 kbar to 200 kbar.

Experiments to measure the permittivity change have been performed on 60 deg orientation sapphire[9] from 20 to 150 kbar with results as shown in Fig. 7. Up to 60 kbar the permittivity is observed to decrease linearly with stress at a rate of 0.078 percent per kilobar. The two higher stress points at 70 and 100 kbar are below the linear extrapolation based on the lower stress data. The current-time waveforms for the higher stresses indicate that conduction is occurring within the sapphire, lowering the current below that predicted from equation (8). Thus, the permittivity change is apparently linear to 100 kbar. At higher stresses we are presently unable to adequately interpret the data in an explicit manner due to the complications of the multiple wave structure resulting from exceeding the Hugoniot elastic limit.

One valuable feature of the shock-wave compression measurement of the permittivity is that the measured current is proportional to the *change* in permittivity. Thus, the shock-wave measurements provide a very sensitive determination of the permittivity change because they do not involve taking the difference between permittivity values obtained at different pressures.

Properties of [111] Germanium

Recently, impact measurements of the resistivity of germanium under shock-wave compression were reported [33, 34]. The technique allowed determination of the resistivity under one-dimensional elastic compression and permitted the identification of the shock-wave pressure induced transition to the white tin structure. Many of the experiments were performed in stress regions for which multiple waves were known to exist due to the cusps in

[9] In an anisotropic crystal, pure longitudinal wave motion is possible only in certain directions called "specific" directions. Although the 60 deg orientation is not theoretically a specific direction for the trigonal system, we have found that under shock-wave compression longitudinal motion is exhibited to a very close approximation. This is not entirely unexpected considering the small variation in elastic constants in the various crystallographic directions.

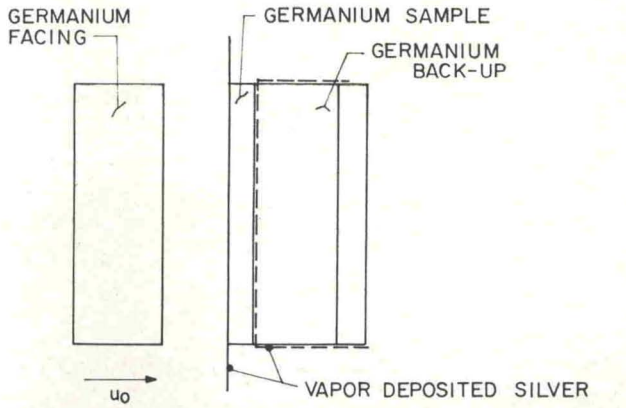

Fig. 8 Experimental arrangement employed to measure the resistance of shock-wave loaded Ge in multiple wave regions

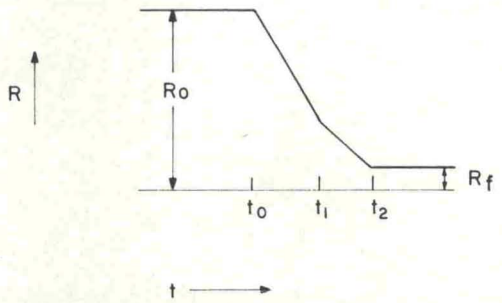

Fig. 9 Expected resistance-time record for a semiconductor exhibiting multiple waves

the stress-volume relation at the Hugoniot elastic limit of 44 kbar and at the 120 kbar high pressure phase transition. Accordingly, the experiments were designed to avoid wave interactions which result if the waves are reflected back into the specimen from an impedance discontinuity.

Again, the shock wave is induced into the sample by the symmetrical impact of [111] orientation germanium disks so that the particle velocity imparted to the specimen is known. With the arrangement as shown in Fig. 8, the resistance between the faces of the specimen disk is then recorded as the shock waves traverse the sample. Backup disks of germanium were carefully mated to the rear of the specimen such that the waves pass through and out of the specimen without reflection.

The propagation of multiple wave fronts divides the specimen into various regions each with a different resistivity and each with a thickness which varies with time depending on the shock velocities. After all the waves have propagated out of the specimen disk, the resistance-time behavior shows a final value, R_f, corresponding to the total stress. The initial unstressed value, R_0, and the final values of resistance are connected by a continuous line consisting of segments of different slope, each segment corresponding to particular wave fronts. This is depicted in Fig. 9 for the case of two wave fronts propagating through the specimen. The resistance-time behavior shows the number of wave fronts (hence the presence of a cusp in the stress-volume relation) and the shock velocity of each wave. However, the division of the total input particle velocity among the various waves is not indicated in the data from a single experiment.

To find the particle velocity associated with each cusp, the impact velocity is varied in small increments around the region of a suspected cusp until a change in the number of waves is observed. This establishes the critical particle velocity of the cusp as accurately as it can be bracketed by the various experiments. In this case, it is particularly important to be able to achieve a preselected velocity. Once the particle velocity associated with the cusp is determined, the stress and velocity for each experiment can be computed. From these measurements

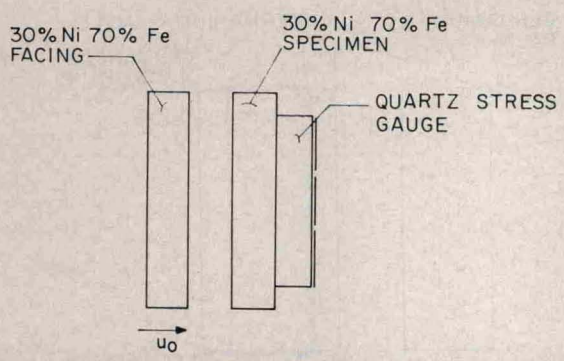

Fig. 10 Experimental arrangement for compressibility measurement on fcc 30 Ni-70 percent Fe

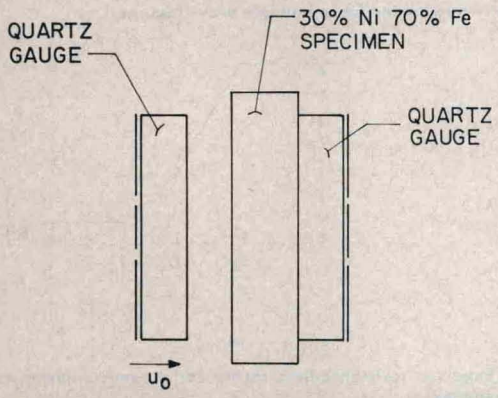

Fig. 11 Experimental arrangement for compressibility measurements employing both impact surface and rear surface measurements of the stress-volume relation

the Hugoniot elastic limit was found to be 44 kbar and the phase transition was found to be at a pressure between 114 and 122 kbar.

Duff and Minshall [35] have demonstrated that the measurement of the shock-wave velocity of a small increment of pressure in the mixed-phase region of a first order transition is sufficient to compute the slope of the pressure-temperature phase line. This unique situation arises because the adiabatic compression resulting from the small pressure increment in the mixed phase region must display a finite compressibility due to the entropy change of the transition. To measure the shock velocity in the mixed phase region, multiple wave reflections and interactions must be avoided and the input stress to the sample must be accurately controlled. This impact experiment is therefore an ideal method for making the measurement. In the mixed phase region of the 120 kbar germanium transition the slope of the phase line was found to be -3.1×10^{-2} kbar deg C^{-1}. This value allows the transition to be identified as the statically observed transition to the white tin structure [34].

With the capability of performing experiments in small pressure increments it is not difficult, although it was not done in this case, to determine the volume change associated with the first order transition. The measurement of the slope of the phase line and the volume change completely specifies the transition since the entropy change of the transition can be calculated from the Clausius-Clapeyron relation.

The results of the resistivity determinations are fully reported elsewhere [34]. They can be summarized by saying that meaningful measurements were obtained only in the elastic region and that the values showed agreement with the theoretical predictions for silicon on the effect of one-dimensional strain on the band structure.

Second Order Transition in 30 Ni-70 Percent Fe

Alloys of about 30 Ni-70 percent Fe in the fcc phase have long been noted for the enormous pressure sensitivity of their magnetic properties. Compressibility determinations for this alloy were recently reported from 4 to 50 kbar which have resulted in an identification of a pressure induced ferromagnetic Curie point transition [36]. Compressibility measurements can be made quite accurately with shock-wave loading techniques and impact experiments have the control necessary to examine the compressibility in enough detail to detect the transition.

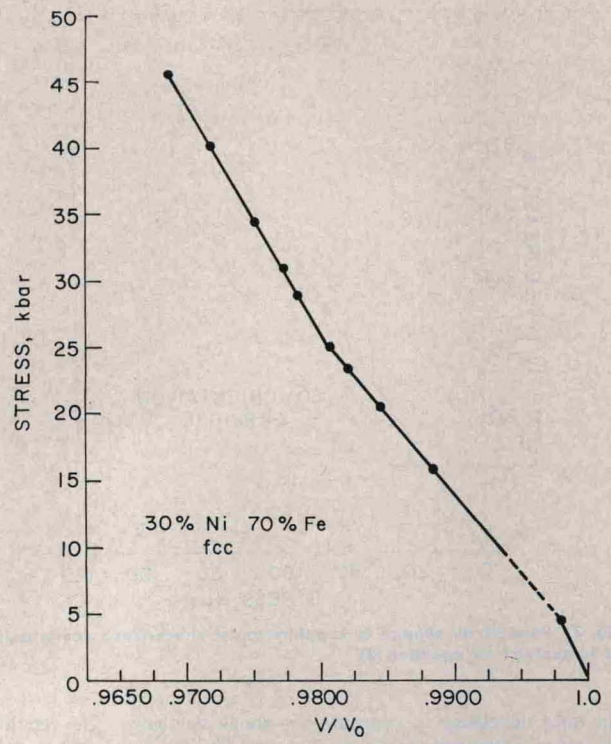

Fig. 12 Stress-volume relation observed for fcc 30 Ni-70 percent Fe

Two different experimental arrangements were used for the compressibility measurements. In one case, see Fig. 10, a symmetrical impact is used to produce a known particle velocity in the sample. The stress-time profile which results after the shock wave has propagated some distance from the impact surface is then measured with a high resolution quartz stress gauge.[10] The time for the shock waves to propagate through the measured thickness is obtained from a measurement of the impact time and the arrival time as indicated by the quartz gauge. These rear surface data alone provide sufficient information to precisely determine the stress and volume change for each experiment. In this case, the additional data on the particle velocity imparted to the sample was used principally for a quantitative comparison with the data measured at the quartz gauge interface. This comparison of the independent measurements of the total particle velocity, which is normally not available in other experiments, serves to give greatly enhanced confidence in the result.

The second method employed is much more elaborate but yields considerably more information. This experiment, which is described in more detail elsewhere [12], is similar to that shown above except that the shock wave is produced by the impact of a quartz gauge. This experimental arrangement is shown in Fig. 11. Provisions are made to obtain the signal from the projectile gauge with the result that the stress and particle velocity are obtained at the impact surface as well as the data ordinarily obtained at the rear surface of the specimen disk. Thus, with this experimental arrangement two completely independent sets of measurements are made on each experiment. This unique capability of directly measuring the shock-wave properties with two entirely independent methods on the same experiment is a

[10] This gauge was developed as a result of the previously mentioned determination of the piezoelectric properties of shock wave loaded quartz [23].

particularly valuable feature. For these experiments the most complete data were available from the quartz gauge at the rear of the specimen and the impact surface data were used to verify the rear surface data.

The stress-volume relation obtained is shown in Fig. 12. As is anticipated for a second-order phase transition, a well-defined change in compressibility is observed at 25 kbar. The cusp at 4 kbar is the Hugoniot elastic limit. In order to accurately determine the critical stress at the transition it was again essential to have the capability of achieving preselected impact velocities in the immediate vicinity of the transition

The results and their interpretation have been fully reported elsewhere [36]. In summary, however, it was possible to identify the sharp change in compressibility as a pressure induced ferromagnetic to paramagnetic transition with values in agreement with the extrapolation of previous lower pressure results. From the Ehrenfest relation, it was also possible to calculate the change of specific heat and thermal expansion at the transition from the measured change in compressibility and the pressure coefficient of Curie temperature.

Summary

The measurements described here were accomplished with various experimental arrangements chosen to obtain maximum utility from the capabilities, of the impact experiment. These capabilities taken individually are valuable and, more significantly, when combined, provide new experimental capability which is especially well suited for the study of the physical properties of solids under shock-wave loading. From a consideration of these measurements utilizing impact techniques and a comparison with measurements which seem possible with explosive loading experiments, the new experimental conditions which characterize impact experiments can be summarized as follows:

1 The impact experiment is a conceptually simple, easily repeated experiment which imparts well-defined input conditions to a specimen.

2 The impact experiment provides virtually continuous values of stress for application to a specimen.

3 By utilizing the symmetrical impact condition, experimental arrangements are possible which provide intimate connection between the measurement of the applied stress and the measurement of the stress induced physical property change.

4 The symmetrical impact condition and the velocity control permit more flexibility in choosing experimental arrangements which avoid the serious wave interaction problems inherent in free surface velocity experiments.

5 The lower limit of the stress range available for investigation is lowered to a few kilobars.

For the measurements performed to date the most useful and definitive data were obtained in the elastic range, which for brittle anisotropic materials extends to high stresses. Within the elastic range the one-dimensional strain configuration imposed by shock-wave compression allows determination of physical property changes resulting from large deformation along specific crystallographic directions. Unfortunately, except for compressibility determination, the experiments conducted for stresses in excess of the elastic limit have not yielded precise well-defined data. The desirable experimental conditions described above are also supplemented by practical considerations of safety and low electrical noise levels.

With these experimental conditions, it has been possible to measure physical properties under large compressions which complement measurements made under static high pressures. The measurements reported are extensive and diverse, and the techniques are well enough developed, such that it seems likely that impact techniques will play an increasingly important role in the study of the properties of solids under large compression.

Acknowledgment

The author is indebted to G. E. Ingram for technical assistance in developing the various experimental arrangements and to numerous Sandia Laboratory colleagues for suggestions and discussions.

References

1 Rice, M. H., McQueen, R. G., and Walsh, J. M., "Compression of Solids by Strong Shock Waves," *Solid State Physics*, Vol. VI, Seitz and Turnbull, eds., Academic Press, New York, 1958.

2 Duvall, G. E., "Some Properties and Applications of Shock Waves," *Response of Metals to High Velocity Deformation*, Shewmon and Zackay, eds., Interscience, New York, 1961.

3 Duvall, G. E., and Fowles, G. R., "Shock Waves," *High Pressure Physics and Chemistry*, Vol. II, Bradley, R. S., ed., Academic Press, New York, 1963.

4 Alder, B. J., "Physics Experiments with Strong Pressure Pulses" *Solids Under Pressure*, Paul and Warschauer, eds., McGraw Hill, New York, 1963.

5 McQueen, R. G., "Laboratory Techniques for Very High Pressures and the Behavior of Metals Under Dynamic Loading," *Metallurgy at High Pressures and High Temperature*, Gschneidner, Hepworth, and Parlee, eds., Gordon and Breach, New York, 1964.

6 Al'tshuler, L. V., "Use of Shock Waves in High-Pressure Physics" *Soviet Physics*, Uspekhi, Vol. 8, 1965, pp. 52–91.

7 Deal, W. E., Jr., "Dynamic High-Pressure Techniques," *Modern Very High Pressure Techniques*, Wentorf, R. H., Jr., ed., Butterworths, Washington, 1962.

8 Doran, D. G., "Measurement of Shock Pressures in Solids," *High Pressure Measurement*, Giardini and Lloyd, eds., Butterworths, Washington, 1963.

9 Hughes, D. S., Gourley, L. E., and Gourley, M. F., "Shock Wave Compression of Iron and Bismuth," Journal of Applied Physics, Vol. 32, 1961, p. 624.

10 Lundergan, C. D., and Herrmann, W., "Equation of State of 6061-T6 Aluminum at Low Pressures," *Journal of Applied Physics*, Vol. 34, 1963, p. 2046.

11 Thurnborg, S., Ingram, G. E., and Graham, R. A., "Compressed Gas Gun for Controlled Planar Impacts Over a Wide Velocity Range," *Review of Scientific Instruments*, Vol. 35, 1964, p. 11.

12 Halpin, W. J., Jones, O. E., and Graham, R. A., "A Submicrosecond Technique for Simultaneous Observation of Input and Propagated Impact Stresses" *Dynamic Behavior of Materials*, ASTM Special Technical Publication No. 336, ASTM, Philadelphia, 1963.

13 Linde, R. K., and Schmidt, D. N., "Measuring the Submicrosecond Response of Shock Loaded Materials," *Review of Scientific Instruments*, Vol. 37, 1966, p. 1.

14 Taylor, J. W., and Rice, M. H., "Elastic-Plastic Properties of Iron," *Journal of Applied Physics*, Vol. 34, 1963, p. 364.

15 Graham, R. A., Ingram, G. E., and Ingram, W. D., "Performance of a High-Velocity Propellant Gun for Controlled Impacts," Sandia Corporation Research Report, SC-4652 (RR), Nov. 1961.

16 Wasley, R. J., and O'Brien, J. F., "Low Pressure Hugoniots of Solid Explosives," Fourth Symposium on Detonation held at the U. S. Naval Ordnance Test Station, Oct. 1965.

17 Ingram, G. E., "Application of Charged Coaxial Cables to the Measurement of Projectile Velocity and Impact Time in a Compressed Gas Gun," *Review of Scientific Instruments*, Vol. 36, 1965, p. 458.

18 Barker, L. M., and Hollenbach, R. E., "System for Measuring the Dynamic Properties of Materials," *Review of Scientific Instruments*, Vol. 35, 1964, p. 742.

19 Graham, R. A., "Piezoelectric Behavior of Impacted Quartz," Abstract, in *Bulletin of the American Physical Society*, Vol. 5, 1960, p. 511.

20 Graham, R. A., "Piezoelectric Behavior of Impacted Quartz," *Journal of Applied Physics*, Vol. 32, 1961, p. 555.

21 Graham, R. A., "A Technique for Studying Piezoelectricity Under Transient High Stress Conditions," *Review of Scientific Instruments*, Vol. 32, 1961, p. 1308.

22 Graham, R. A., "Dielectric Anomaly in Quartz for High Transient Stress and Field," *Journal of Applied Physics*, Vol. 33, 1962, p. 1755.

23 Graham, R. A., Neilson, F. W., and Benedick, W. B., "Piezoelectric Current from Shock-Loaded Quartz—A Submicrosecond Stress Gauge," *Journal of Applied Physics*, Vol. 36, 1965, p. 1775.

24 Karcher, J. C., "A Piezoelectric Method for the Instantaneous Measurement of High Pressures," Scientific Papers of the Bureau of Standards, No. 445, 1922.

25 Wackerle, J., "Shock-Wave Compression of Quartz," *Journal of Applied Physics*, Vol. 33, 1962, p. 922.

26 Fowles, G. R., "Shock-Wave Compression of Quartz," Doctoral Thesis, Department of Geophysics, Stanford University, 1962.

27 Koga, U., Aruga, M., and Yoshinaka, Y., "Theory of Plane Elastic Waves in a Piezoelectric Crystalline Medium and Determination of Elastic and Piezoelectric Constants of Quartz," *Physical Review*, Vol. 109, 1958, p. 1467.

28 Bechmann, R., "Elastic and Piezoelectric Constants of Alpha-Quartz," *Physical Review*, Vol. 110, 1958, p. 1060.

29 Jones, O. E., "Piezoelectric Behavior of Quartz Shock-Loaded at 79 K," Abstract in *Bulletin of the American Physical Society*, Vol. 11, 1966, p. 414.

30 Halpin, W. J., "Current from a Shock-Loaded Short Circuited Ferroelectric Ceramic Disk," *Journal of Applied Physics*, Vol. 37, 1966, p. 153.

31 Graham, R. A., and Ingram, G. E., "Capacitance Change of Sapphire Under Shock-Wave Compression—A Shock-Wave Stress Gauge," Abstract in *Bulletin of the American Physical Society*, Vol. 11, 1966, p. 414.

32 Brooks, W. P., and Graham, R. A., "Shock-Wave Compression of Sapphire," Abstract in *Bulletin of the American Physical Society*, Vol. 11, 1966, pp. 414.

33 Graham, R. A., Jones, O. E., and Holland, J. R., "Shock-Wave Compression of Germanium From 20 to 140 Kbar," *Journal of Applied Physics*, Vol. 36, 1965, p. 3955.

34 Graham, R. A., Jones, O. E., and Holland, J. R., "Physical Behavior of Germanium Under Shock-Wave Compression," *Journal of the Physics and Chemistry of Solids*, Vol. 27, 1966, p. 1519.

35 Duff, R. E., and Minshall, S. F., "Investigation of a Shock-Induced Transition in Bismuth," *Physical Review*, Vol. 108, 1957, p. 1207.

36 Graham, R. A., Anderson, D. H., and Holland, J. R., "Shock-Wave Compression of 30 Ni–70 Percent Fe Alloys—The Pressure Induced Magnetic Transition," *Journal of Applied Physics*, Vol. 38, 1967, p. 223.

Supplementary References on Mechanical Properties Determined by Impact Techniques.

37 Barker, L. M., Lundergan, C. D., and Herrmann, W., "Dynamic Response of Aluminum," *Journal of Applied Physics*, Vol. 35, 1964, p. 1203.

38 Butcher, B. M., and Canon, J. R., "Influence of Work-Hardening on the Dynamic Stress-Strain Curves of 4340 Steel," *American Institute of Aeronautics and Astronautics Journal*, Vol. 2, 1964, p. 2174.

39 Hartman, W. F., "Determination of Unloading Behavior of Uniaxially Strained 6061-T6 Aluminum from Residual Strain Measurements," *Journal of Applied Physics*, Vol. 35, 1964, p. 2090.

40 Barker, L. M., and Hollenbach, R. E., "Interferometer Technique for Measuring the Dynamic Mechanical Properties of Materials," *Review of Scientific Instruments*, Vol. 36, 1965, p. 1617.

41 Halpin, W. J., and Graham, R. A., "Shock-Wave Compression of Plexiglas from 3 to 20 Kbar," Fourth Symposium on Detonation held at U. S. Naval Ordnance Laboratory, Oct. 1965.

42 Butcher, B. M., and Karnes, C. H., "Strain-Rate Effects in Metals," *Journal of Applied Physics*, Vo.. 37, 1966, p. 402.

43 Barker, L. M., Butcher, B. M., and Karnes, C. H., "Yield Point Phenomenon in Impact-Loaded 1060 Aluminum," *Journal of Applied Physics*. Vol. 37, 1966, p. 1989.

Reprinted from the December 1967
Journal of Basic Engineering

Issued by
Technical Information Division III
Sandia Corporation
Albuquerque, New Mexico